



**HAL**  
open science

# Rapid identification of bast fibers in ancient handmade papers based on improved characterization of lignin monomers by Py-GCxGC/MS

Bin Han, Yimin Yang, Bo Wang, Hongen Jiang, Michel Sablier

► **To cite this version:**

Bin Han, Yimin Yang, Bo Wang, Hongen Jiang, Michel Sablier. Rapid identification of bast fibers in ancient handmade papers based on improved characterization of lignin monomers by Py-GCxGC/MS. *Cellulose*, 2023, 30, pp.575-590. 10.1007/s10570-022-04924-9 . hal-03920838

**HAL Id: hal-03920838**

**<https://hal.science/hal-03920838>**

Submitted on 3 Jan 2023

**HAL** is a multi-disciplinary open access archive for the deposit and dissemination of scientific research documents, whether they are published or not. The documents may come from teaching and research institutions in France or abroad, or from public or private research centers.

L'archive ouverte pluridisciplinaire **HAL**, est destinée au dépôt et à la diffusion de documents scientifiques de niveau recherche, publiés ou non, émanant des établissements d'enseignement et de recherche français ou étrangers, des laboratoires publics ou privés.

# Rapid identification of bast fibers in ancient handmade papers based on improved characterization of lignin monomers by Py-GCxGC/MS

Bin Han<sup>1</sup>, Yimin Yang<sup>1</sup>, Bo Wang<sup>2</sup>, Hongen Jiang<sup>1</sup>, Michel Sablier<sup>3</sup>

<sup>1</sup>*Department of Archaeology and Anthropology, School of Humanities, University of Chinese Academy of Sciences, 100049 Beijing, China*

<sup>2</sup>*Xinjiang Uygur Autonomous Region Museum, 830000 Urumchi, China*

<sup>3</sup>*Centre de Recherche sur la Conservation (CRC, USR 3224), Muséum national d'Histoire naturelle, Ministère de la Culture et de la Communication, CNRS, 75005 Paris, France.*

Corresponding Authors: [michel.sablier@mnhn.fr](mailto:michel.sablier@mnhn.fr)

**ABSTRACT:** The precise identification of hemp (*Cannabis sativa* L.) fiber in ancient papers is of great significance in the study of paper history. However, different species of phloem fibers belonging to bast fibers (e.g., hemp, ramie, flax, jute) used in traditional hand papermaking in the East Asian region present similar microscopic morphological traits, which renders their accurate identification problematic and may cause controversy in archaeological interpretations. In this study, a method for the precise identification of Cannabis fiber in ancient handmade papers by Py-GCxGC/MS was developed for rapid fiber characterization in ancient papers. The proposed approach was based on the separation of characteristic lignin monomers from lignocellulose by Py-GCxGC/MS, with an example of joss paper samples excavated from the archaeological site of Astana tombs dating to the Tang Dynasty. The bidimensional chromatographic separation of the pyrolysis signature of plant materials allows a well-structured layout in the 2D chromatograms. Therefore, it becomes possible to distinguish these different plant materials by applying a multivariate analysis treatment to the lignin monomers. The improved GCxGC separation of lignin monomers showed the benefit of the GCxGC profile for lignin monomer group identification as well as for the application of statistical analysis. The developed method presents the advantages of being rapid and effective for archaeological and cultural heritage applications in necessitating a tiny quantity of sample.

*Keywords lignin, pyrolysis, comprehensive gas chromatography/MS, fiber identification, Astana site*

## INTRODUCTION

Ancient papers are of high cultural value as carriers for the information that can be decoded from their contents for historical and paleographical studies (Helman-Ważny, 2016; Sakamoto and Okada, 2013). Apart from their traditional use: writing support, painting support, administrative and official applications, paper has been used in specific applications such as joss paper (ghost money, Figure 1, Figure S1 in the Supplementary information) in rituals and ceremonies that greatly promoted cultural diversity in societal development (Han et al., 2021; Scott, 2007; Seaman, 1982). Nevertheless, the material source of ancient joss paper has seldom been reported to hinder a comprehensive knowledge of paper offerings as a unique oriental cultural phenomenon in ancient China and neighboring regions (Blake, 2011; Kwon, 2007; McCreery, 1990).

The art of traditional East Asian papermaking resides in the rational choice of fibers, which constitutes an opportunity to chronologically and geographically locate the origin of paper if a reliable analytical method is available. In fact, fiber identification of ancient papers has been in practice since the beginning of the 19<sup>th</sup> century (Briquet, 1886; Wiesner, 1887); nevertheless, accurate plant fiber identification still remains problematic and sometimes causes controversy (Bergfjord et al., 2010; Drege, 1986; Kvavadze et al., 2009). For instance, archaeological fiber characterization commonly uses microscopy for their identification, while some fibers have quite similar morphological traits (e.g., hemp, ramie, flax and jute). Consequently, concerns have been raised about the risk of analysis resulting in distorted archaeological interpretations (Haugan and Holst, 2014; Lukesova and Holst, 2021).

The preservation conditions of archaeological fibers as well as typically nondestructive or micro destructive requirements limit the application of some analytical techniques in forming a rapid fiber identification in ancient papers (Martoglio et al., 1990). On-line pyrolysis hyphenated with gas chromatography/mass spectrometry (Py-GC/MS) is among the most frequently used techniques for fiber material studies due to a simple preparation of the samples with minimum quantities required and, consequently, has rooted cultural heritage applications (Degano et al., 2018; Nacci et al., 2022; Shedrinsky et al., 1989). Py-GC/MS has been successfully explored to define new criteria for characterizing plant fibers commonly used in East Asian handmade papers based on the characterization of different sets of plant markers (phytosterols and terpenoids) in a defined region of interest (ROI) from the pyrolysis of East Asian paper samples (Avataneo and Sablier, 2017; Han et al., 2019; Han et al., 2021).

However, it has been observed that some bast fibers found in plant materials (e.g., hemp, flax, ramie, jute) have fewer markers in the ROI, a situation that poses difficulties for their comparison by the established ROI approach (Han et al., 2019). Although it has been observed that the lignin components, such as the ratio of syringyl- to guaiacyl-units (S/G ratio (del Río et al., 2004; Ohra-Aho et al., 2013; Silva et al., 2012)) among bast fibers vary (Marques et al., 2010; Pandey, 2007), the large quantity consumed with efficient sample preparation is not always suitable for cultural heritage applications where tiny quantities are the rules (Alves et al., 2009; Alves et al., 2006; Nanayakkara et al., 2016). The raw fiber material of the lignocellulosic complex has also been pyrolyzed, while poor chromatographic separation of lignocellulose mixtures has been observed and caused problems in the integration of lignin peak derivatives (Chen et al., 2017; Lima et al., 2008; Nunes et al., 2010).

The development of multidimensional gas chromatography offered potentialities for better separation and higher resolution helpful in the analysis of complex chemical systems (Chin and Marriott, 2014; Tranchida et al., 2015). In fact, the application of GCxGC separation for the investigation of cultural heritage materials, e.g., handmade papers and inks (Han et al., 2016; Perruchini et al., 2022), lacquers (Han et al., 2022; Okamoto et al., 2018), organic residue (Brychova et al., 2021; Cnuts et al., 2018; Lebedev et al., 2021; Umamaheswaran et al., 2022), and bone collagen (Cersoy et al., 2018; Dutta et al., 2020), has demonstrated the benefits of using an analytical method of higher selectivity with a quicker and more reliable identification procedure compared to 1D GC/MS analysis (Han et al., 2018). Coupling of pyrolysis to GCxGC/MS demonstrated its efficiency in distinguishing paper fibers difficult to differentiate by microscopy, especially those from the Moraceae and Thymelaeaceae families, which produce different groups of markers in the ROI (Avataneo and Sablier, 2017; Han et al., 2016; Han et al., 2018; Han et al., 2017; Han et al., 2019). However, to date, the identification for those with rare markers in ROI (Han et al., 2019), such as plants showing bast fibers (e.g., hemp, ramie, flax, jute), remains problematic (Haugan and Holst, 2014; Lukesova and Holst, 2021). The GCxGC separation of lignin monomers in East Asian handmade papers may have its characteristic potentials while it has not been explored.

With the aim of investigating the GCxGC separation features of lignocellulose and exploring the potential of analyzing lignin monomers in East Asian handmade papers for their potential as discriminating markers, this study explores the efficiency of Py-GCxGC/MS for the separation and detection of lignin monomers for an improved characterization and data treatment workflow. The 2D separation of individual lignin monomers as well as grouping

features of lignin markers were examined and scrutinized. Rapid and effective bast fiber identification in archaeology and cultural heritage studies by pyrolysis-comprehensive two-dimensional gas chromatography is for the first time developed based on the improved characterization of lignin monomers.

## **EXPERIMENTAL SECTION**

### **Materials.**

Modern reference handmade paper samples from hemp, ramie, jute, and flax papers were first analyzed in duplicate to acquire the chemical profiles of lignin monomers. The archaeological samples used in this study consisted of paper offerings excavated from Astana cemetery (Figure S2). This complex was located on the famous Silk Road, which is particularly well known for its abundant unearthed mummies, written documents, textiles, plant remains, and food residues (Chen et al., 2022; Chen et al., 2014). The tombs cover an area of approximately 10 km<sup>2</sup> and served as a public graveyard for the ancient Gaochang people, dating from approximately the 3<sup>rd</sup> to the 9<sup>th</sup> centuries. The tombs where the samples (Figure 1) were unearthed were built in the early period of the Tang Dynasty (618-907 AC) according to the written documents buried within the tombs.

### **Microscopic observation.**

Direct microscopic observation of the fragment surface was conducted with a digital microscope (VHX-600, Keyence). The observation was conducted in reflection mode. For fiber analysis, a small amount of fibers from the clean part of the fragment was taken with cleaned dissecting needles and placed on the surface of a microslide with a drop of distilled water to disperse the fibers. The iodine-zinc chloride stain reagent was then added to the fiber preparation and covered with a cover glass. The prepared slide was observed under a stereomicroscope.

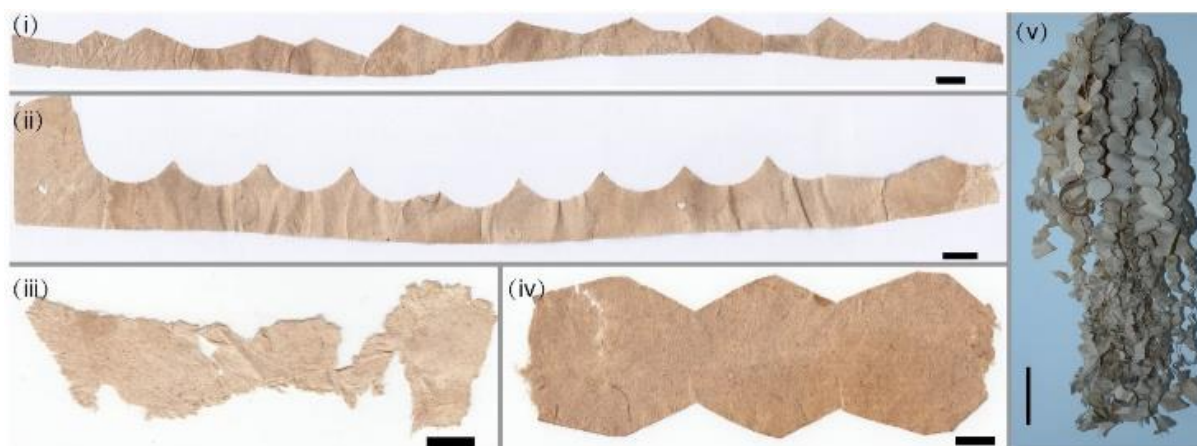


**Fig. 1** The archaeological paper offering samples from Astana cemetery. (i) offcut of paper offerings from the tomb of 72TAM184:5; (ii) offcut of paper offerings from the tomb of 72TAM184:2; (iii) remains of paper offerings from the tomb of 73TAM501:108; (iv) paper offerings from the tomb of 73TAM518:9; (v) general view of paper offerings from Astana Cemeteries. scale bar in (i)-(ii) is 1 cm, in (v) is 10 cm.

### **Py-GCxGC/MS Analysis.**

Py-GCxGC/MS analysis was conducted with a Shimadzu QP 2010 Ultra mass spectrometer (Shimadzu, Champs-sur-Marne, France) equipped with a two-stage thermal modulator ZX 2 (Zoex, Houston, USA). Pyrolysis was performed using a vertical micro-furnace-type pyrolyzer PY-3030D (Frontier Lab, Fukushima, Japan) directly connected to the injection port of the gas chromatograph. The quadrupole mass spectrometer was operated at  $20,000 \text{ u.s}^{-1}$ , with a scan range from 50 to 500 u, using electron ionization at 70 eV. Data processing of the 2D raw data was achieved using GC Image software, version 2.4 (Lincoln, Nebraska). Identification of components was performed by comparing the mass spectra of unknown components with reference compounds from the NIST MS library (2011) and interpretation of the main fragmentations. Full experimental details are given in the Supplementary information.

### **Data pretreatment and PCA/cluster analysis.**

Compound identification and peak integration in the total ion chromatogram (TIC) of Py-GCxGC/MS data were performed using GC Image software, version 2.4 (Lincoln, Nebraska). The TIC peak areas (either raw or normalized values) were used as responses for multivariate data analysis to explore the most characteristic features of each paper sample. After the data pretreatment procedure, the data were subjected to exploratory principal component analysis (PCA). The PCA analyses and hierarchical clustering analysis were performed using

Unscrambler X (Version 10.4) software from CAMO Software AS (Oslo, Norway). A full description of the data treatment procedure is given in the Supplementary information. Briefly, in the process of PCA modelling, data were centered, and different variable weighting parameters were used. Here, weight as  $1/STD$  is defined as the standard deviation calculated among each variable while the data were mean centered. Regarding clustering analysis, the default Euclidean distance measure was used.

## RESULTS AND DISCUSSION

### **Dilemma in identifying ancient bast paper fibers by microscopy and ROI plant markers.**

As seen from Figure 1 and Figure 2, samples (i) and (ii) are comparatively thin with distortion. The surface contains black protuberances, large phloem fibers and clustered fibers on the surface, which have also been observed in contemporary handmade papers (Arnaud-Nguyen, 2020). Sample (iii) is similar to sample (i) in thickness and morphology but with more flexibility. Sample (iv) also has a rough morphology with twisted and clustered fibers and large plant phloem.

Figure 3 displays the morphological features of stained fibers from the investigated paper offerings of Astana cemeteries. The color of the stained fibers from the paper offerings varies from wine red to pink when stained by Hertzberg reagent. The fibers in sample (i) and sample (iv) generally have a variable thickness along their length, with cross striations at certain intervals forming the nodes, a shape characteristic of bast fibers such as hemp, ramie, mulberry and paper mulberry. Longitudinal striations, a diagnostic feature for hemp and ramie fibers, are recognizable, although they were likely worn due to the pulping process. The fibers in sample (ii) and sample (iii) resemble fibers in sample (iv) with cross striations and longitudinal striations but are of comparatively constant thickness along their length. Parenchymal cells or coarse serrated cells, which are usually seen in bamboo, rice, and wheat straw, were not observed here and allowed us to rule out those as fiber sources (Figure S3).

The process of cutting may cause comparative straight fracture, while ramming and/or pulping left the trace of obvious swelling fibers and degrees of fibrillation. Evidence of fibrillation was observed in all samples, indicating a process of manual ramming or pulping (Figure S3-S4,

Supplementary information). No chemical reaction between iodine solution and starch grains from sizing was noticed in the process of fiber staining, indicating the absence of starch sizing treatment.

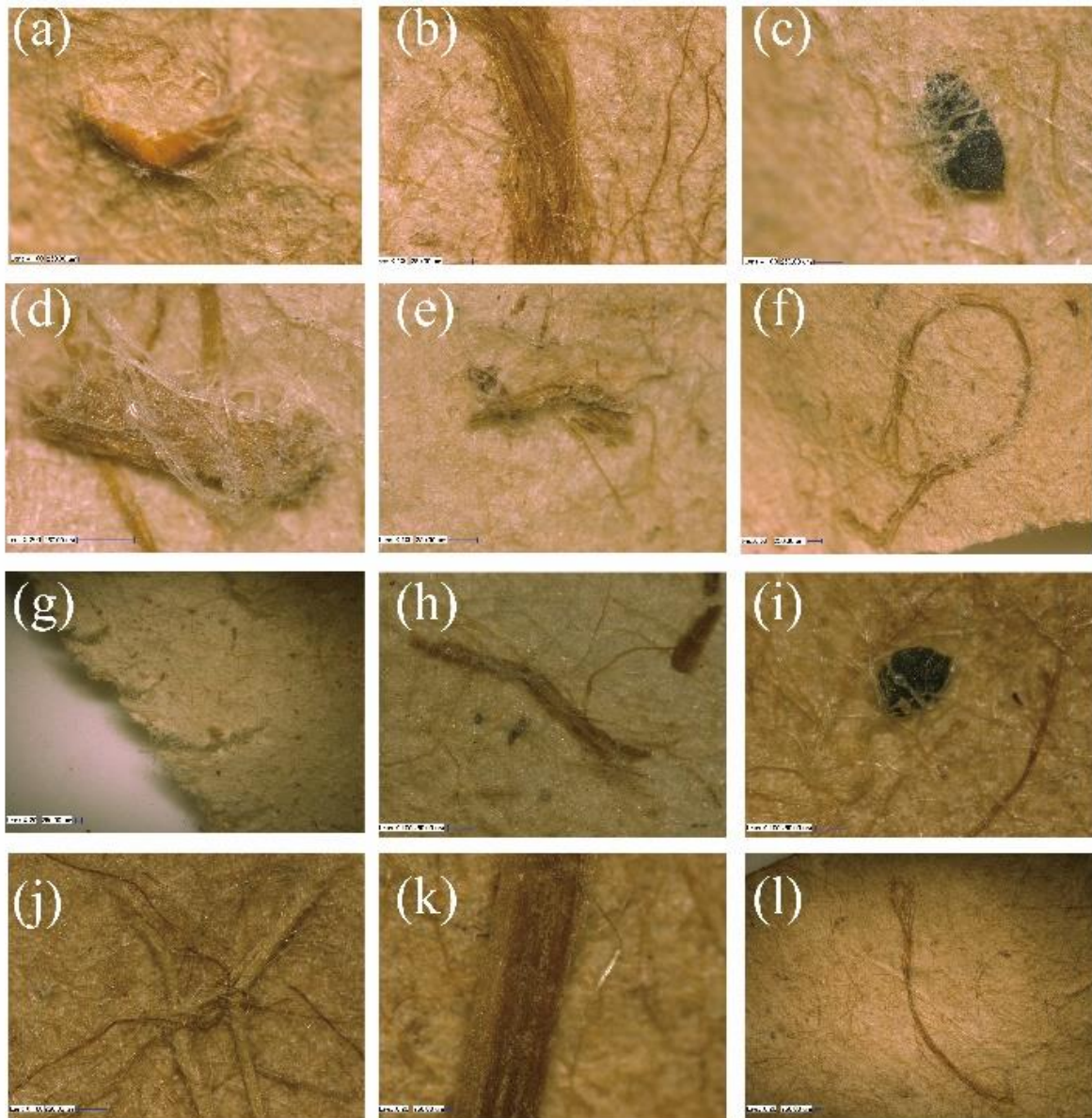


**Fig. 2** Micrograph of paper offerings from Astana tombs. (i) 72TAM184:5, (a)-(b); (ii) 72TAM184:2, (c)-(f); (iii) 72TAM501:108, (g)-(h); (iv) 73TAM518:9, (i)-(l).

Considering a microscopic approach, the Hertzberg stain is a quick way to have a rough estimation of the lignin content in the fibers indicated by the color presentation of the stained fibers. For instance, the complex phenolic polymer lignin plays a decisive role in the presence of fiber color when stained by Herzberg reagent. Previous studies in fiber identification have examined the content of lignin changing from significantly low (0–5% of dry weight in hemp,

ramie, and cotton) to low (8–15% of dry weight in mulberry and paper mulberry trees) to low-to-moderate (15–20% of dry weight in rice and wheat straw) to high (25–30% of dry weight in bamboo) (Shi and Li, 2013). This change in lignin content may make the observed fiber take on the color of wine red, pink, blue, blue-grey, and yellow, accordingly. However, its precision (resolution) may not be enough to measure minor and varied differences in the lignin content (Figure S5, Supplementary information), and the color representation may be affected by other compositions in the paper structures.

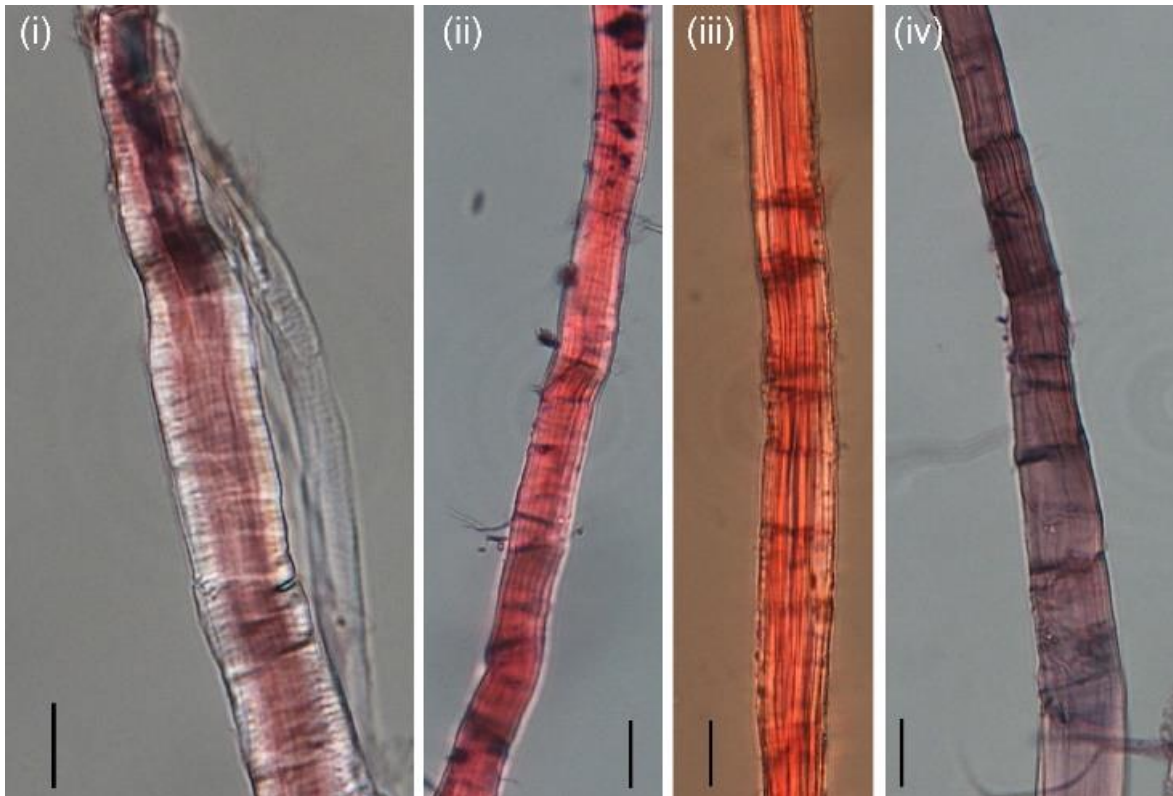


**Fig. 3** Microscopic morphological features of the stained fibers of samples (i)-(iv), scale bar=20  $\mu\text{m}$ . More microscopic pictures examined in the course of the present work can be found in Figure S3, Supplementary information.

On the other hand, one must emphasize that, during the microscopic observation of fiber morphological traits in the aim of their identification, difficulties can be encountered in relation to the modifications during their preparation for papermaking, which makes their characterization more difficult: a case is well known for the distinction of hemp and ramie fibers (Haugan and Holst, 2014; Lukesova and Holst, 2021). Moreover, in Figure 3(i), questionable discrepancies are visible, while Figure 3(iv) bottom shows an enlarged fiber structure of no help for the assignment. Any further separation based only on microscopic observation poses a certain risk of misidentification for the reasons stated above (Haugan and

Holst, 2014; Lukesova and Holst, 2021). Although microscopic observations suggest the possible use of bast fiber materials in Astana samples, microscopic analysis alone makes it difficult to make more accurate identification to differentiate fibers showing similar morphological traits (Haugan and Holst, 2014; Lukesova and Holst, 2021).

We further conducted Py-GC/MS analysis to check the plant markers in the defined region of interest (ROI) following the analytical approach described previously (Avataneo and Sablier, 2017), but few marker peaks were observed in the resulting pyrograms, impinging the assignment of fiber origin with satisfying reliability (Figure S6, Table S1 and Table S2). Referring to the previous investigation of East Asian paper samples, the present situation is consistent with bast fiber papers revealing a low level of characteristic structures (Han et al., 2019). However, one must concede that the lack of plant markers (phytosterol and terpenes) does not lead to reliable identification of the fiber's material.

All the dilemmas in precisely identifying bast fibers suggest a complementary approach to find a more reliable criterion. As a result, we explored the separation and quantification of lignin monomers by Py-GC<sub>x</sub>GC/MS as a needful supplement in the precise characterization of these bast paper fibers.

### **The GC<sub>x</sub>GC separation of lignocellulose components and the grouping features of lignin monomers from handmade papers.**

Lignin is composed of polymers of phenylpropane  $\beta$ -aryl ether structure units, a polyphenol structure produced by oxidative condensation of three phenylpropanoid monomers: *p*-coumaryl, coniferyl and sinapyl alcohols. The phenyl moieties of such compounds differ in the hydroxy and methoxy substituents in the *p*-hydroxyphenyl, guaiacyl and syringyl units (abbreviated with the acronyms H-, G- and S-units, respectively, Figure S7). The content, distribution and ratio of the three phenyl units (in particular for S/G) in different plant species varies noticeably (Figure S7), a characteristic pattern that can be used to discriminate different wood and fibers (Wang et al., 2021).

Lignin and polysaccharides are bound through covalent bonds and form lignocellulose. The analysis of lignin monomers (with different H/S/G types) in handmade papers was observed to be present as minor compounds often coeluting with cellulose pyrolysis products during 1D Py-GC/MS analysis, a point that makes both their identification and quantification difficult (Avataneo and Sablier, 2017). In contrast, thanks to the potential of bidimensional GC<sub>x</sub>GC

separation, it is favorably observed that the lignin monomers were separated from carbohydrates in the resulting chromatograms, as exemplified in Figure 4. The first- and second-dimensional separations in GCxGC separation are independent, which yields in theory orthogonal results in such a way that constituents of similar properties (volatility and polarity) will be displayed in ordered structures: classes of similar compounds showing up as clusters or groups of compounds more or less aligned (Ramos and Udo, 2009). This chromatographic layout greatly simplifies chemical class recognition and compound identification in the case of a complex mixture, such as the one represented in the case of cellulose and lignin. If a strict orthogonality is barely attained in practice, it must be emphasized that the choice of column for the second dimension is a key factor for separation efficiency: noticeably, the increased aryl content of the second column in the present experiment increases the capacity to separate aromatic structures (expected from lignin) from other analytes (like cellulose derivatives). On the basis of previous pyrolysis of lignin contents of several plant materials (del Río et al., 2011; Galletti and Bocchini, 1995; Van Erven et al., 2017), 27 potential lignin markers (Table 1) were chosen for the assignment of lignin content of reference samples of handmade papers of hemp, ramie, jute and flax, as well as for the four samples of Astana paper. As previously observed in comparing Py-GC/MS analysis of paper plant fiber materials and traditional handmade paper samples, typical markers from the raw materials are generally more numerous than the manufactured samples (Avataneo and Sablier, 2017): the same observation applies here, and for this reason, the number of lignin markers detected in the paper samples may appear more limited compared to direct analysis of the raw lignin material (Del Rio et al., 2009). The basic structures of these markers are reported in Figure S9 (Supplementary information), while the detection of these 27 lignin markers during Py-GCxGC/MS analysis of the samples is reported in Table 1 for the four reference papers of hemp, ramie, flax and jute. As noted above, the ordered structured features of lignin monomers consist of a common phenol structure and different substituted groups: a common alcohol/methoxy structure with substituted R (Figure 4b), a point suitable to explore the benefits of GCxGC separation for chromatographic separation (Groenewold et al., 2017; Netzel, 2019). As seen in Table 1, hemp presented most of these markers, while ramie and flax were characterized by an almost total disappearance of them, particularly guaiacyl and syringyl compounds, an observation in accordance with the expected value of the S/G ratio reported elsewhere in the literature.

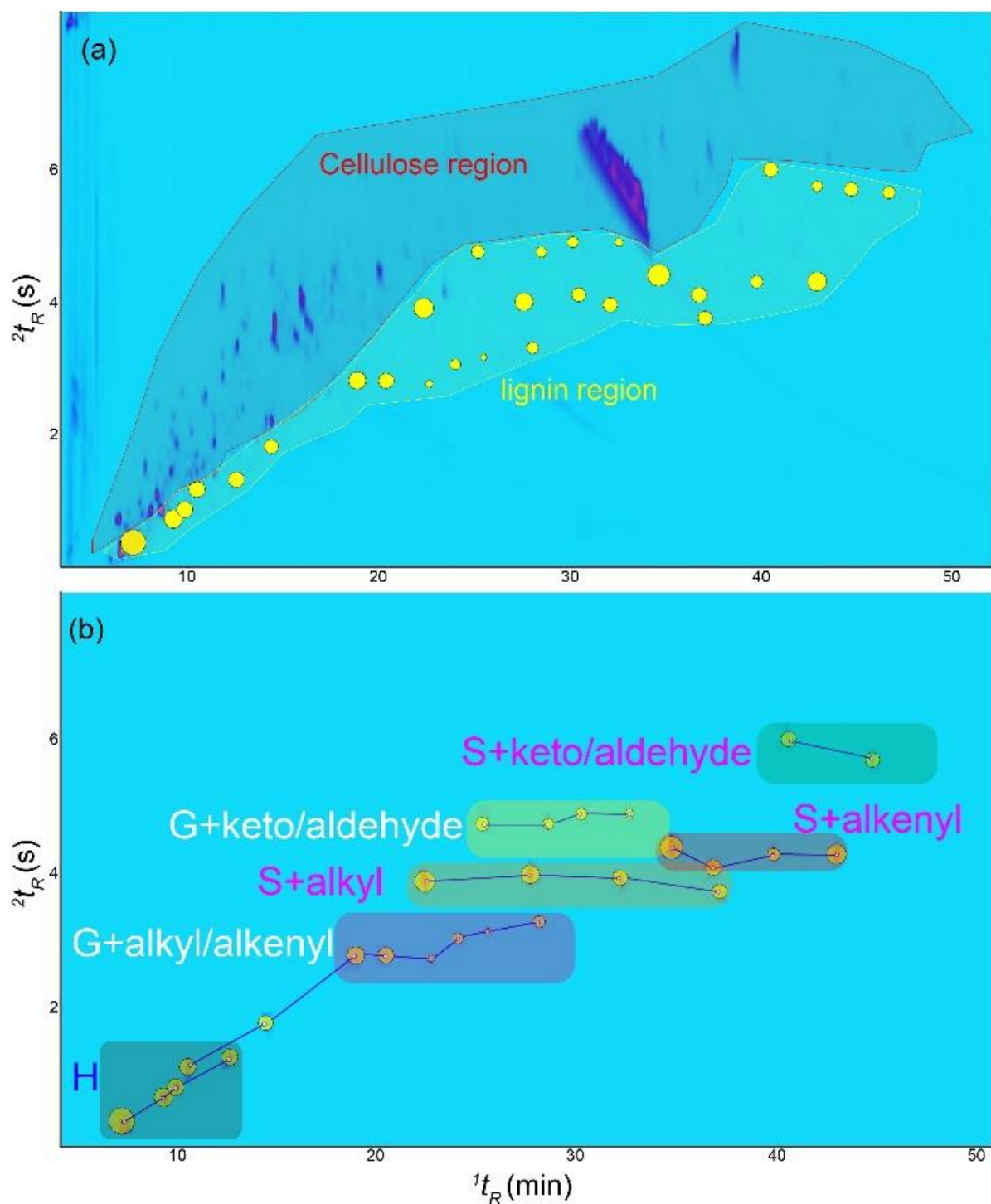


**Fig. 4** (a) An example of a 2D chromatogram resulting from the pyrolysis of a handmade reference jute paper showing the separation of the lignocellulose components, (b) the grouping features of different series of lignin monomers (H,G,S monomers with different side-chains) in the 2D chromatogram space. In (a), the cellulose region represents a region providing mainly cellulose pyrolysis products, and the lignin region represents a region providing mainly lignin pyrolysis products. In (b), H, G, and S represent different types of lignin monomers, while alkyl, alkenyl, keto-/aldehyde/enol represent side-chain constituents. The full 2D chromatographic space is shown in Figure S8. In (a) and (b), the yellow blobs represent the lignin monomers, and for compound identification, refer to Table 1 and Figure S9.

## Advances of rapid GCxGC screening of lignin monomers for handmade paper discrimination.

The detection of lignin markers in Table 1 confirms that ramie and flax reference papers provided comparatively fewer lignin monomers than hemp and jute reference papers. In particular, if the H-type monomers were present, G-type and S-type monomers almost disappeared during analysis since only some monomers, such as G3 and G4, were detected during Py-GCxGC/MS analysis of these two ramie and flax reference paper samples. In contrast, jute and hemp reported a high number of lignin markers detected during pyrolysis, as shown in Table 1. Considering the presence of these lignin markers, Py-GCxGC/MS chromatograms of the reference paper samples and the Astana paper samples were used to compile the integral of the corresponding peaks of interest among the 27 lignin markers chosen (Table 1). Figure 6 reports the measured ratio of S/G-type monomers from the integration of peak values of the corresponding compounds in the 2D chromatograms normalized to the sum of the peak areas.

**Table 1.** List of lignin marker compounds detected in the 2D chromatogram of the Py-GCxGC/MS analysis of the reference paper samples of hemp, ramie, flax and jute with their respective retention times in the two dimension ( $^1t_R$ ,  $^2t_R$ ), molecular weight (MW), main peaks in the corresponding mass spectrum (base peak in bold), formula, identification and presence in the reference samples.

NO.	$^1t_R$	$^2t_R$	MW	m/z	formula	identification	origin <sup>a</sup>	hemp	ramie	flax	jute
H1	7.55	0.35	94	<b>94</b> ,66,65,95,93	C <sub>6</sub> H <sub>6</sub> O	phenol	H	x	x	x	x
H2	9.65	0.7	108	<b>108</b> ,107,77,79,90	C <sub>7</sub> H <sub>8</sub> O	2-methylphenol	H	x	x	x	x
H3	10.25	0.85	108	<b>108</b> ,107,79,77,51	C <sub>7</sub> H <sub>8</sub> O	4-methylphenol	H	x	x	x	x
H4	12.95	1.3	122	<b>107</b> ,122,77,79,94	C <sub>8</sub> H <sub>10</sub> O	2,6-dimethylphenol	H	x	x	x	x
G1	10.85	1.15	124	<b>109</b> ,124,81,95,53	C <sub>7</sub> H <sub>8</sub> O <sub>2</sub>	guaiacol	G	x			x
G2	14.75	1.8	138	<b>138</b> ,123,95,67,55	C <sub>8</sub> H <sub>10</sub> O <sub>2</sub>	p-methylguaiacol	G	x			x
G3	19.25	2.8	152	<b>137</b> ,152,91,77,138	C <sub>9</sub> H <sub>12</sub> O <sub>2</sub>	4-ethylguaiacol	G	x	x	x	x
G4	20.75	2.8	150	<b>150</b> ,135,77,107,79	C <sub>9</sub> H <sub>10</sub> O <sub>2</sub>	4-vinylguaiacol	G	x	x	x	x
G5	23	2.75	164	<b>164</b> ,103,107,55,91	C <sub>10</sub> H <sub>12</sub> O <sub>2</sub>	p-eugenol	G	x			
G6	24.35	3.05	166	<b>137</b> ,166,81,151,55	C <sub>10</sub> H <sub>14</sub> O <sub>2</sub>	p-propylguaiacol	G	x		x	x
G7	25.85	3.15	164	<b>164</b> ,77,103,55,91	C <sub>10</sub> H <sub>12</sub> O <sub>2</sub>	isoeugenol	G	x			x
G8	28.4	3.3	164	<b>164</b> ,149,77,121,91	C <sub>10</sub> H <sub>12</sub> O <sub>2</sub>	trans-Isoeugenol	G	x			x

G9	25.55	4.75	152	152,151,81,53,109	C <sub>8</sub> H <sub>8</sub> O <sub>3</sub>	vanillin	G	x		x
G10	28.85	4.75	166	137,166,81,122,82	C <sub>10</sub> H <sub>14</sub> O <sub>2</sub>	homovanillin	G	x	x	x
G11	30.5	4.9	166	151,166,123,108,52	C <sub>9</sub> H <sub>10</sub> O <sub>3</sub>	acetovanilone	G	x	x	x
G12	32.9	4.9	180	137,180,122,138,94	C <sub>10</sub> H <sub>12</sub> O <sub>3</sub>	guaiacylacetone	G	x		x
G13	36.5	4.85	180	137,180,124,77,91	C <sub>10</sub> H <sub>12</sub> O <sub>3</sub>	cis-coniferyl alcohol	G	x		
S1	22.7	3.9	154	154,139,93,96,65	C <sub>8</sub> H <sub>10</sub> O <sub>3</sub>	2,6-dimethoxyphenol	S	x		x
S2	27.95	4.0	168	168,153,125,53,65	C <sub>9</sub> H <sub>12</sub> O <sub>3</sub>	2,6-dimethoxy-4-methylphenol	S	x		x
S3	32.45	3.95	182	167,182,77,107,124	C <sub>10</sub> H <sub>14</sub> O <sub>3</sub>	2,6-dimethoxy-4-ethylphenol	S	x		x
S4	43.25	5.75	196	167,196,101,99,168	C <sub>11</sub> H <sub>16</sub> O <sub>3</sub>	2,6-dimethoxy-4-propylphenol	S	x		x
S5	35	4.4	180	180,165,137,77,91	C <sub>10</sub> H <sub>12</sub> O <sub>3</sub>	2,6-dimethoxy-4-vinylphenol	S	x		x
S6	37.1	4.1	194	194,91,119,103,147	C <sub>11</sub> H <sub>14</sub> O <sub>3</sub>	2,6-dimethoxy-4-allylphenol	S	x		x
S7	40.1	4.3	194	194,91,119,103,147	C <sub>11</sub> H <sub>14</sub> O <sub>3</sub>	cis-2,6-dimethoxy-4-propenylphenol	S	x		x
S8	43.25	4.3	194	194,91,119,103,147	C <sub>11</sub> H <sub>14</sub> O <sub>3</sub>	trans-2,6-dimethoxy-4-propenylphenol	S	x		x
S9	40.85	6	182	182,181,93,65,79	C <sub>9</sub> H <sub>10</sub> O <sub>4</sub>	syringaldehyde	S	x		x
S10	45.05	5.7	196	181,196,153,182,67	C <sub>10</sub> H <sub>12</sub> O <sub>4</sub>	acetosyringone	S	x		x

<sup>a</sup> H phenol unit, G guaiacol unit, S syringol unit. G1 and G2 are not used in the S/G calculation and PCA (Figure 8) due to their area variation.

As shown in Figure 5, the most intensive lignin content (in considering measured values for the S/G ratio) was observed for the jute reference paper, largely differentiated from the others by its ratio lying at approximately 5.0. As a result, jute could be clearly differentiated from the other reference paper samples of hemp, ramie and flax using the lignin content expressed by the S/G ratio. In accordance with the present results, the lignin structure of jute fibers was previously reported to predominantly release syringol units correlated to a relatively high observed S/G ratio during Py-GC/MS analysis (Del Rio et al., 2009). Moreover, numerous investigations on the lignin content of jute are in accordance with the predominance of syringyl lignin units over guaiacol lignin units (del Río et al., 2004; Islam and Sarkanen, 1993). Clearly, the measured S/G ratio for the jute reference sample through Py-GCxGC/MS analysis does not invalidate it. However, the measured S/G ratio for jute in Figure 5, is always noticeably higher than those of hemp, ramie and flax, was slightly higher than the previously reported values in the literature. The observed tendency of low S/G values for hemp, flax and ramie reference papers compared to jute reference paper concurs with what is currently reported for these bast fibers (del Río et al., 2004; del Río et al., 2011). In addition, considering the values of the S/G

ratio associated with the flax and ramie reference paper samples and the high value for the jute reference paper sample, the measurement of the S/G ratio in the 2D chromatograms is proven to be a potential tool useful to differentiate paper samples among those manufactured from bast fiber plant materials with the minimum quantity required ( $\mu\text{g}$  range) for heritage and archaeology applications.

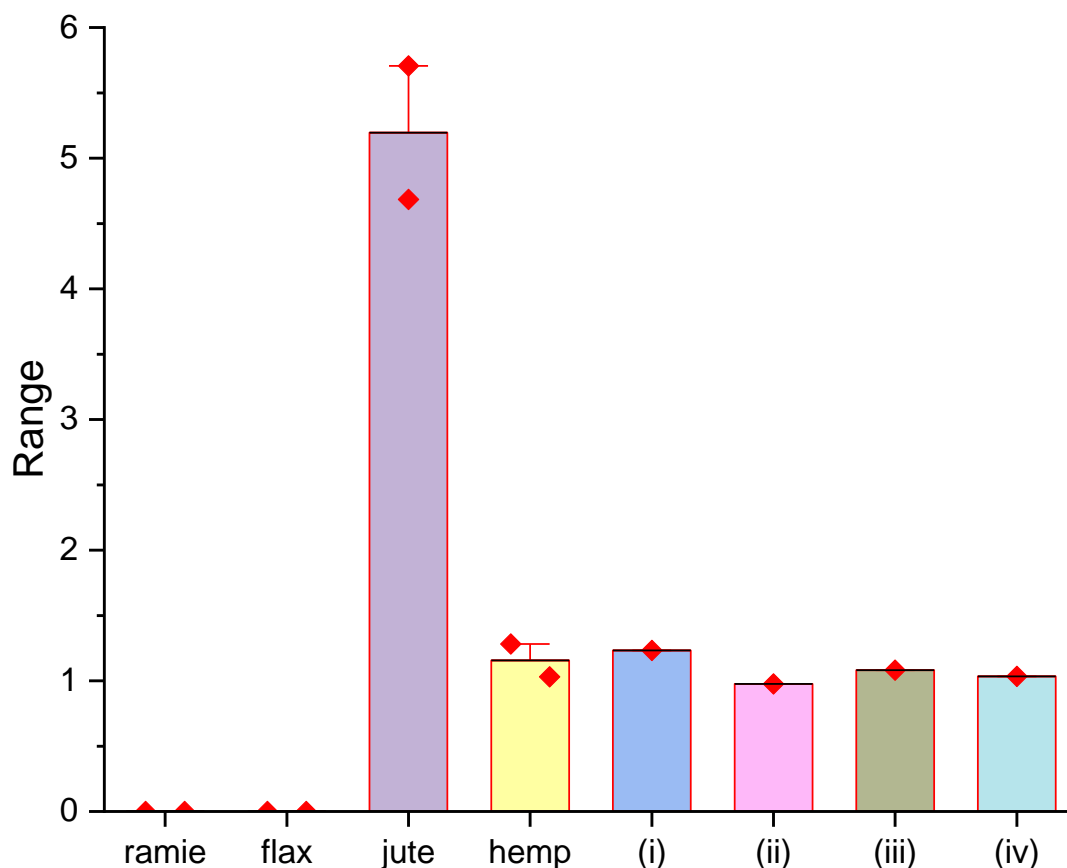


**Fig. 5** Measured S/G ratio by Py-GCxGC/MS for the reference samples of ramie, flax, hemp, jute and the four Astana samples (i)-(iv).

Reported fiber lignin contents in hemp and jute are higher than those of flax (del Río et al., 2004), even if consideration must be made for the role of the region of the stem analyzed, the stage of development, and the environmental conditions of growth. Noticeably, the S/G ratio of the outer plant tissues at the origin of fiber material for papermaking is likely subject to variation between the flowering and seed maturation stages of the plant. Depending on the technique of traditional papermaking, and especially on the period of the year chosen for extracting fibers from the plants, one can expect slight variation in these ratios. However, one must keep in mind that traditional East Asian handmade papermaking is an elaborated craftwork using rough retting techniques resulting in the preparation of fiber material for

papermaking that could be significantly different from the techniques applied in modern pulp production. Indeed, the content and composition of the lignin components could be different from those expected under modern chemical extraction procedures. As shown in Figure 5, the known tendency in S/G ratio variations of fiber species: jute>hemp>flax, ramie, are respected and can therefore be considered for sample comparison: jute and hemp reference papers can be differentiated from ramie and flax reference papers, which both showed disappearance of syringol compounds in the resulting chromatograms (Table 1).

From the above experimental results, by comparison, the four Astana paper samples can be differentiated (i) on one side from the jute reference sample, since the S/G ratio in this latter case is noticeably higher than those of the Astana samples, measured between 0.98 and 1.23, (ii) on the other side from the ramie and flax reference papers that showed the absence of compounds associated with syringol units in the chromatograms. Concomitantly, the S/G ratio for the hemp reference sample 1.03-1.28 was closer to the above values for the Astana paper samples. This similarity was interpreted as a hemp origin for the fiber material in use in the making of the Astana paper samples. At this stage of development, these results based on the ratios between S/G markers confirmed those obtained from microscopic analysis (see above) and placed the measurement of S/G ratio as an advantageous supplementary approach.

For the analysis of lignin content in fibers, the molar ratio of syringaldehyde to vanillin was also considered for the analysis of jute fibers (Islam and Sarkanen, 1993). The ratios of these two lignin markers were taken into account for comparison between hemp reference paper samples and Astana paper samples. If one considers vanillin (G9) and syringaldehyde (S9) pyrolysis products associated to G and S lignin subunits, respectively, as it is admitted for the chemical characterization of tissue lignin after chemical degradation of labile ether linkages ( $\beta$ -O-4' and  $\alpha$ -O-4), the corresponding ratios syringaldehyde/vanillin (S9/G9) in both reference hemp paper (mean value= 0.73) and the four Astana paper samples (mean value= 0.71) appeared to be very close. Notably, chemical methods for the characterization of lignin in plant tissues revealed that, in the case of flax, calculation of the quantity of lignin monomers released per g unit of lignin may vary to some extent, raising the potential role of fiber maturation (Day et al., 2005). If, as underlined above, consideration is taken to the retting techniques of fiber preparation, reasonably, pyrolysis will not simplify the conclusion that can be drawn from the observation of syringaldehyde to vanillin ratios. However, one can concede that similarity in the measured ratios evolves in the sense of a similarity between reference samples and

unknowns, as it is the case here for the reference hemp paper sample and the four Astana paper samples.

Multivariate data analysis of the pyrolysis of reference paper samples and Astana paper samples was conducted. Both cluster hierarchical and principal component analyses were performed on the integral of peaks assigned to lignin markers in the 2D chromatograms. Figure 6 reports the dendrogram of hierarchical cluster analysis of the reference paper samples and the four Astana paper samples considering normalized raw data for peak integration. As shown in Figure 6, the closest distance between Astana paper samples and reference paper samples appeared for the hemp reference paper origin. The jute reference paper presents the highest distance to Astana paper samples, while ramie and flax reference paper lies at an intermediate distance. In accordance with the previous values of the S/G ratio, hierarchical cluster analysis of the reference paper samples and the four Astana paper samples confirms the closest similitude of Astana paper samples with a hemp fiber origin.

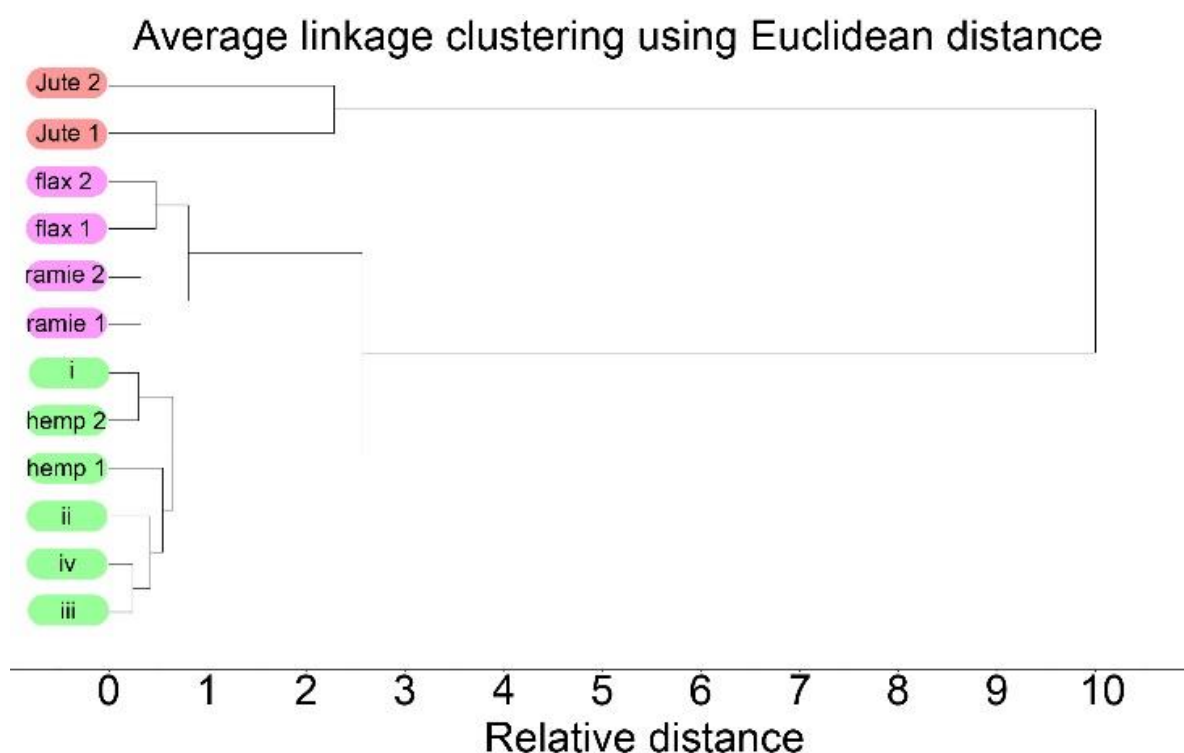


**Fig. 6** Dendrogram of the hierarchical clustering of reference paper samples and Astana paper samples using normalized data of the 27 lignin markers reported in Table 1.

Figures 7 and 8 report the corresponding score plots and loading plots for the analysis of the experimental results obtained by Py-GCxGC/MS considering the 27 lignin markers listed in Table 1. Figure 7 reports these results considering all the markers, and Figure 8 reports these

results considering only the G-type and S-type markers. During the treatment of data, it has appeared that weighting by 1/standard deviation (STD) provided the most efficient results for the PCA since, by definition, the normalization to 1/STD is introduced to minimize the potential effect of high concentration lignin markers. Moreover, a variable of positioning, namely, the S/G ratio reported as C1, was added to the data for PCA treatment. In both cases, the score plots express the similarity between samples through the clustering of their projection on the axis representative of the grouping of data. In addition, data selection for the G- and S-type monomers contributed to increasing the data presentation on the cluster of archaeological samples through their projections on PC1 and PC2.

On the scores plot in Figure 7, grouping of paper samples can be summarized with a nice clustering distribution of four reference papers of ramie and flax, jute, and hemp, and a loose clustering of Astana archaeological paper samples. To further interpret the PCA results, the loading plots express the relative contributions of H-, G- and S-type monomers to the distribution of paper samples in the scores plot. In Figure 7, (i) the ramie and flax reference paper samples ( $S/G=0$ ) present a high contribution of H-type monomers, which locates them on the left space on the score plot: the high percentage of H1 and H2 monomers for ramie paper and H3, G4, and G6 monomers for flax paper in the data matrix help to discriminate these two papers although their distances are relatively close; (ii) the combination of C1 (S/G ratio) and G- and S-type lignin markers accounts for the distribution of jute and hemp reference papers as well as the Astana archaeological papers on the right side of the score plot. The jute reference paper sample that showed a high S/G ratio (C1) presents a high contribution of S-type monomers; (iii) the hemp reference sample and the four Astana paper samples present a high contribution of G-type monomers.

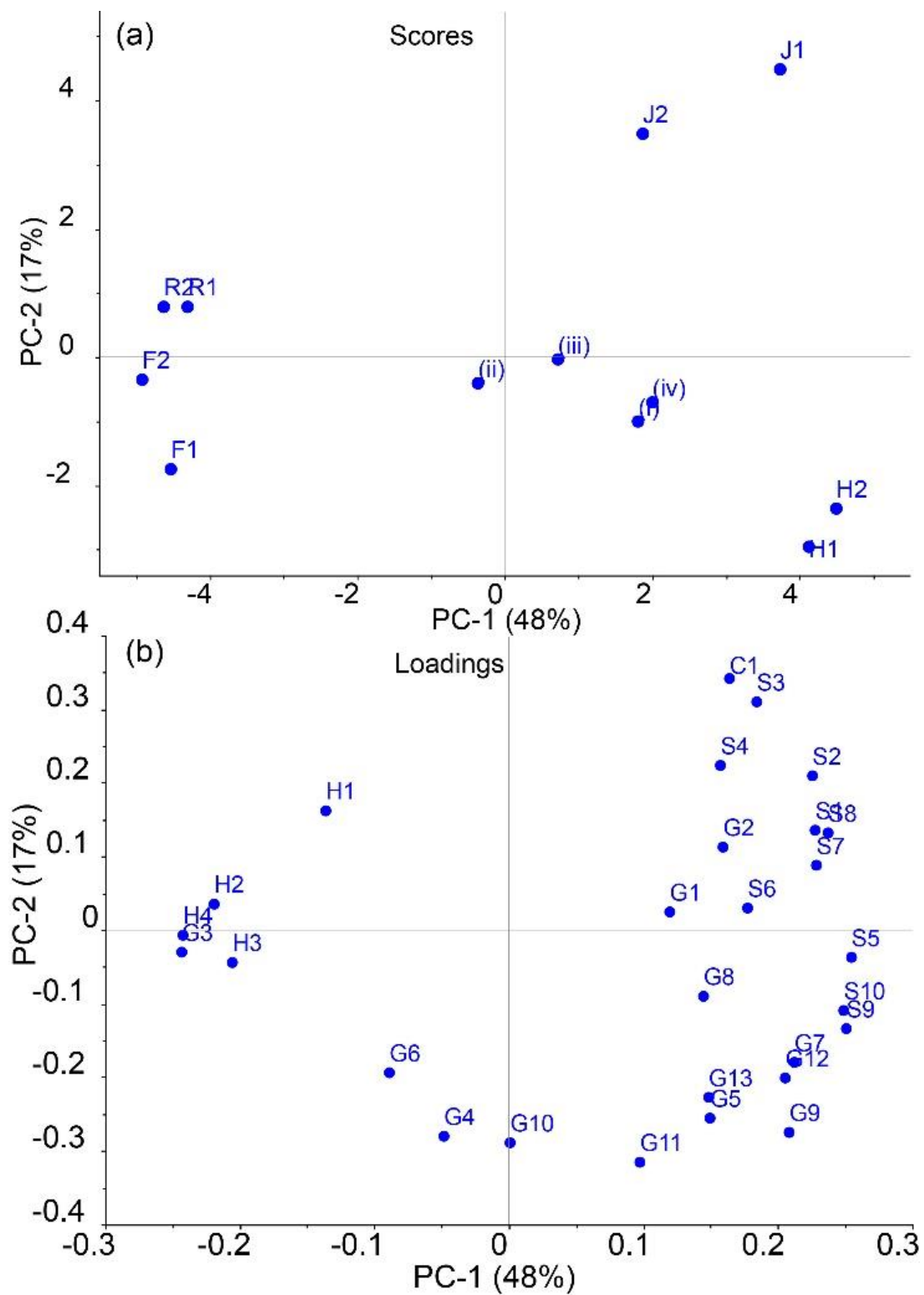


**Fig. 7** PCA (weighted as 1/STD) of the reference paper samples and the Astana paper samples using normalized values for the 27 lignin markers (Table 1). In (a), R: ramie, F: flax, J: jute, H: hemp, (i)-(iv): the four Astana paper samples; in (b), H/G/S represents the three types of lignin monomers.

These results are concordant with the calculated S/G ratio of each analysis associated with the different paper samples since ramie and flax reference paper samples with their S/G=0 were well differentiated from the two other reference paper samples, hemp and jute, as well as the four Astana paper samples. The loose distribution of the archeological samples showing unclear cluster discrimination between jute and hemp reference paper also demonstrates that the evident difference in the S/G ratio (Figure 5) has been weakened in the PCA using 1/STD modelling.

In view of the loadings plot of Figure 7, results were further modelled with only G- and S-type lignin monomers. Similarly, in Figure 8, (i) a high G-type contribution makes the flax and ramie reference paper samples stand out from the others, while G3 and G4 for ramie paper and G6, G10, and G11 for flax paper make them locate on the upper and lower sides in the left space; (ii) the jute reference paper samples always present the same high contribution of S-type monomers, and C1 stands out as a discriminative factor; and (iii) while the hemp reference paper sample and the four Astana paper samples present a high contribution from G-type monomers, these two last characteristics are well correlated to the value of the respective S/G ratio.

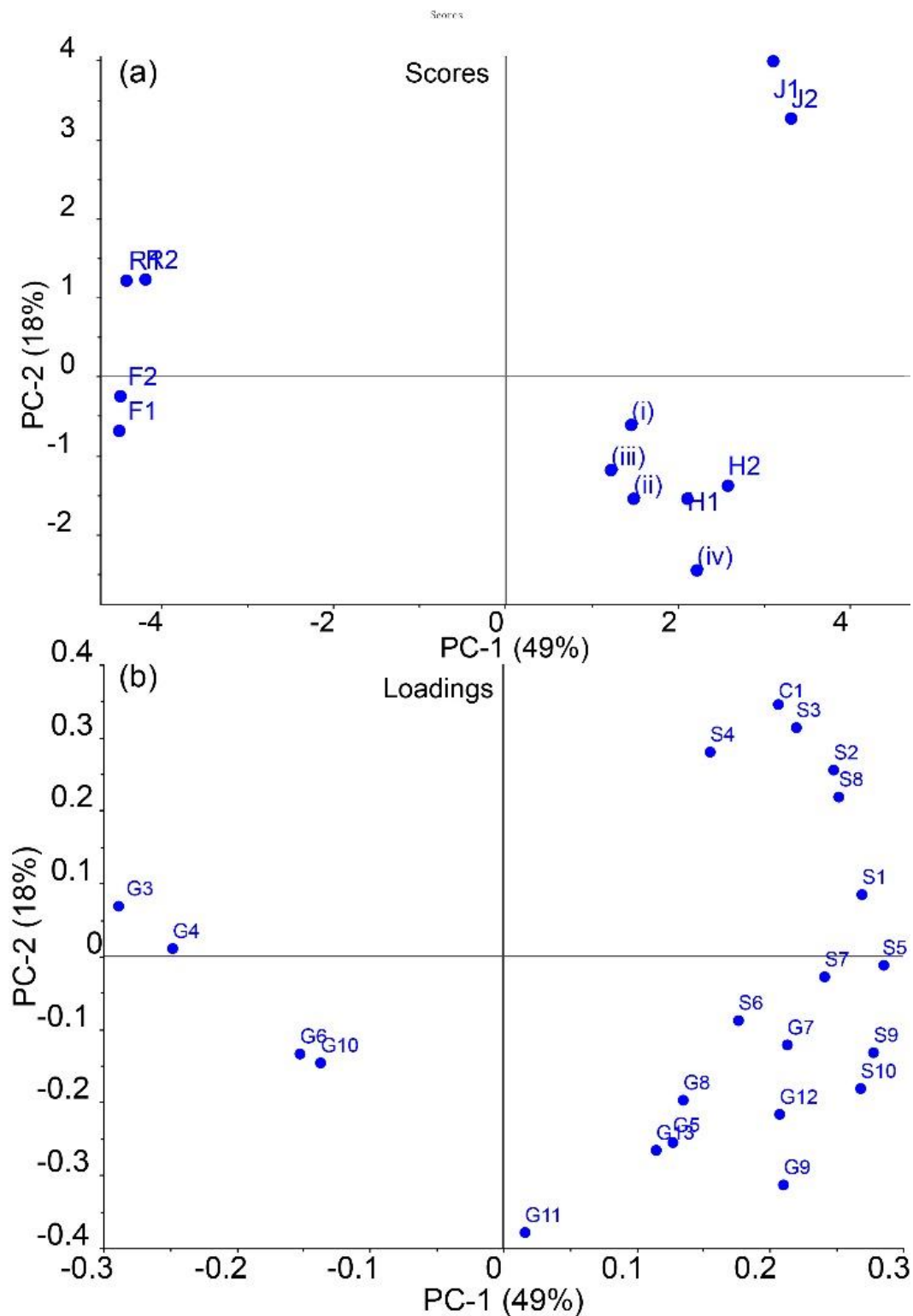


**Fig. 8** PCA of the reference paper samples and the Astana paper samples using normalized values for the only G-type and S-type lignin markers (Table 1), weighted as  $1/STD$ . In (a), R: ramie, F: flax, J: jute, H: hemp, (i)-(iv): the four Astana paper samples; in (b), H/G/S represents the three types of lignin monomers.

As stated above for the measurement of the S/G ratio from data extracted from the Py-GCxGC/MS chromatograms and hierarchical cluster analysis, these PCA data confirm the closest similitude of Astana paper samples with hemp paper, leading to the conclusion that the excavated Astana paper samples are of hemp origin for its fiber material. Considering the relative ratio of each lignin marker among the 27 lignin markers chosen, PCA permits us to visualize the variability between reference paper samples and allows us to ultimately deduce the highest similarity of the four Astana paper samples with the hemp reference paper. Moreover, the validity of this statement lies in spite of the variability observed in the distribution of data points for the reference samples hemp, ramie, flax, and jute. In particular, the results confirm that the first PC nicely differentiates hemp paper on one side from ramie and flax papers on the other side, while the second PC quite equally differentiates jute paper from hemp, and flax from ramie papers.

## **CONCLUSION**

Benefiting from 2D separation, a rapid method has been explored for the characterization and identification of bast fibers using lignin monomers. Pertinency of this approach has been demonstrated with a set of joss paper samples excavated from the archaeological site of Astana tombs dating to the early period of the Tang Dynasty (618-907 AC). The pyrolysis sampling reduced the required quantity to a minimum amount (in the  $\mu\text{g}$  range), and bidimensional gas chromatography allows an effective separation of the lignin monomers from the lignocellulose with grouping features in the 2D space distribution: the direct pyrolysis of handmade papers under Py-GCxGC/MS conditions favors their characterization and permits further data treatment based on multivariate data analysis. This new method with a simple procedure placed lignin pyrolysis products as potential biomarkers for the characterization of ancient papers and fabric materials in archaeology and cultural heritage applications.

These analytical characterizations permit us to explore Cannabis fiber utilization as a papermaking source along the Silk Road in a situation where little information is currently known about early papermaking and usage activities. The use of paper offerings by Astana residents in ceremonial contexts reflects the influence of interior areas as a means of cultural communication along the Silk Road. The new analytical strategy proposed here will have

promise in solving key problems in precise fiber assignment and identification for archaeological interpretations.

## **ACKNOWLEDGMENTS**

The authors thank Dr. Sakamoto Shouji for providing some of the reference paper samples and Mr. Vilmont Léon-Bavi for the help in the paper fiber analysis.

## **Declarations**

## **Funding**

B.H. is grateful to the national social science fund for their financial support (No. 19CKG029).

## **Conflict of interest**

The authors have no conflicts of interest to declare that are relevant to the content of this article.

## **Ethical standards**

This article is an original work not submitted to/published elsewhere in any form or part. Proper acknowledgement to other works is given and the results are presented clearly, honestly and without fabrication.

## **Ethical approval**

This article does not contain any studies involving human participants or animals performed by any of the authors.

## **Availability of data and material**

Data are available from the corresponding author upon request.

## Author Contributions

The manuscript was written through contributions of all authors, and all authors have given approval to the final version of the manuscript.

## REFERENCES

- Alves A, Gierlinger N, Schwanninger M, Rodrigues J. (2009). Analytical pyrolysis as a direct method to determine the lignin content in wood: Part 3. Evaluation of species-specific and tissue-specific differences in softwood lignin composition using principal component analysis. *J. Anal. Appl. Pyrolysis*, 85(1-2), 30-37. <https://doi.org/10.1016/j.jaap.2008.09.006>
- Alves A, Schwanninger M, Pereira H, Rodrigues J. (2006). Analytical pyrolysis as a direct method to determine the lignin content in wood: Part 1: Comparison of pyrolysis lignin with Klason lignin. *J. Anal. Appl. Pyrolysis*, 76(1-2), 209-213. <https://doi.org/10.1016/j.jaap.2005.11.004>
- Arnaud-Nguyen E. (2020). Paper Analyses of Tocharian manuscripts of the Pelliot Collection stored in the National Library of France (Bibliothèque nationale de France). *Z Badań nad Książką i Księgozbiórami Historycznymi*, 14(3), 385-410. <https://doi.org/10.33077/uw.25448730.zbkh.2020.630>
- Avataneo C, Sablier M. (2017). New criteria for the characterization of traditional East Asian papers. *Environ. Sci. Pollut. Res.*, 24(3), 2166-2181. <https://doi.org/10.1007/s11356-016-6545-0>
- Bergfjord C, Karg S, Rast-Eicher A, Nosch M-L, Mannering U, Allaby R, Murphy B, Holst B. (2010). Comment on “30,000-year-old wild flax fibers”. *Science*, 328(5986), 1634-1634. <https://doi.org/10.1126/science.1186345>
- Blake C F. (2011). *Burning Money: The Material Spirit of the Chinese Lifeworld*. University of Hawaii Press. <https://doi.org/doi:10.1515/9780824860103>
- Briquet C-M. (1886). *Recherches sur les premiers papiers employés en Occident et en Orient du Xe au XIVe siècle*. imprimerie de Daupeley-Gouverneur.
- Brychova V, Roffet-Salque M, Pavlu I, Kyselka J, Kyjakova P, Filip V, Ivo S, Evershed R P. (2021). Animal exploitation and pottery use during the early LBK phases of the Neolithic site of Bylany (Czech Republic) tracked through lipid residue analysis. *Quat. Int.*, 574, 91-101. <https://doi.org/10.1016/j.quaint.2020.10.045>
- Cersoy S, Daheur G, Zazzo A, Zirah S, Sablier M. (2018). Pyrolysis comprehensive gas chromatography and mass spectrometry: A new tool to assess the purity of ancient collagen prior to radiocarbon dating. *Anal. Chim. Acta*, 1041, 131-145. <https://doi.org/10.1016/j.aca.2018.07.048>
- Chen F, Hou B, Chen S, Zhang H, Gong P, Zhou A. (2017). Biochemicals distribution and the collaborative pyrolysis study from three main components of Helianthus annuus stems based on PY-GC/MS. *Renew. Energy*, 114, 960-967. <https://doi.org/10.1016/j.renene.2017.07.083>
- Chen T, Wang B, Jiang H. (2022). New archaeobotanical evidence for Medicago from the Astana Cemetery in Turpan, Xinjiang. *Herit. Sci.*, 10(1), 1-7. <https://doi.org/10.1186/s40494-022-00694-6>
- Chen T, Yao S, Merlin M, Mai H, Qiu Z, Hu Y, Wang B, Wang C, Jiang H. (2014). Identification of Cannabis fiber from the Astana Cemeteries, Xinjiang, China, with reference to its

- unique decorative utilization. *Econ. Bot.*, 68(1), 59-66. <https://doi.org/10.1007/s12231-014-9261-z>
- Chin S-T, Marriott P J. (2014). Multidimensional gas chromatography beyond simple volatiles separation. *Chem. Commun.*, 50(64), 8819-8833. <https://doi.org/10.1039/C4CC02018A>
- Cnuts D, Perrault K A, Stefanuto P-H, Dubois L M, Focant J-F, Rots V. (2018). Fingerprinting Glues Using HS-SPME GC×GC–HRTOFMS: a New Powerful Method Allows Tracking Glues Back in Time. *Archaeometry*, 60(6), 1361-1376. <https://doi.org/10.1111/arcm.12364>
- Day A, Ruel K, Neutelings G, Crônier D, David H, Hawkins S, Chabbert B. (2005). Lignification in the flax stem: evidence for an unusual lignin in bast fibers. *Planta*, 222(2), 234-245. <https://doi.org/10.1007/s00425-005-1537-1>
- Degano I, Modugno F, Bonaduce I, Ribechini E, Colombini M P. (2018). Recent advances in analytical pyrolysis to investigate organic materials in heritage science. *Angew. Chem. Int. Ed.*, 57(25), 7313-7323. <https://doi.org/10.1002/anie.201713404>
- del Río J C, Gutiérrez A, Martínez Á T. (2004). Identifying acetylated lignin units in non - wood fibers using pyrolysis - gas chromatography/mass spectrometry. *Rapid Commun. Mass Spectrom.*, 18(11), 1181-1185. <https://doi.org/10.1002/rcm.1457>
- del Río J C, Rencoret J, Gutiérrez A, Nieto L, Jiménez-Barbero J, Martínez Á T. (2011). Structural characterization of guaiacyl-rich lignins in flax (*Linum usitatissimum*) fibers and shives. *J. Agric. Food. Chem.*, 59(20), 11088-11099. <https://doi.org/10.1021/jf201222r>
- Del Rio J C, Rencoret J, Marques G, Li J, Gellerstedt G, Jimenez-Barbero J, Martinez A T, Gutiérrez A. (2009). Structural characterization of the lignin from jute (*Corchorus capsularis*) fibers. *J. Agric. Food. Chem.*, 57(21), 10271-10281. <https://doi.org/10.1021/jf900815x>
- Drege J-P. (1986). L'analyse fibreuse des papiers et la datation des manuscrits de Dunhuang. *Journal asiatique*, 274(3-4), 403-415. <https://doi.org/10.2143/JA.274.3.2011558>
- Dutta S, Kumar S, Singh H, Khan M A, Barai A, Tewari A, Rana R S, Bera S, Sen S, Sahni A. (2020). Chemical evidence of preserved collagen in 54 - million - year - old fish vertebrae. *Palaeontology*, 63(2), 195-202. <https://doi.org/10.1111/pala.12469>
- Galletti G C, Bocchini P. (1995). Pyrolysis/gas chromatography/mass spectrometry of lignocellulose. *Rapid Commun. Mass Spectrom.*, 9(9), 815-826. <https://doi.org/10.1002/rcm.1290090920>
- Groenewold G S, Johnson K M, Fox S C, Rae C, Zarzana C A, Kersten B R, Rowe S M, Westover T L, Gresham G L, Emerson R M. (2017). Pyrolysis two-dimensional GC-MS of miscanthus biomass: quantitative measurement using an internal standard method. *Energy & Fuels*, 31(2), 1620-1630. <https://doi.org/10.1021/acs.energyfuels.6b02645>
- Han B, Daheur G, Sablier M. (2016). Py-GC×GC/MS in cultural heritage studies: An illustration through analytical characterization of traditional East Asian handmade papers. *J. Anal. Appl. Pyrolysis*, 122, 458-467. <https://doi.org/10.1016/j.jaap.2016.10.018>
- Han B, Fan X, Chen Y, Gao J, Sablier M. (2022). The lacquer crafting of Ba state: Insights from a Warring States lacquer scabbard excavated from Lijiaba site (Chongqing, southwest China). *Journal of Archaeological Science: Reports*, 42, 103416. <https://doi.org/10.1016/j.jasrep.2022.103416>
- Han B, Lob S, Sablier M. (2018). Benefit of the use of GC×GC/MS profiles for 1D GC/MS data treatment illustrated by the analysis of pyrolysis products from east Asian

- handmade papers. *J. Am. Soc. Mass. Spectrom.*, 29(8), 1582-1593. <https://doi.org/10.1007/s13361-018-1953-7>
- Han B, Niang J, Rao H, Lyu N, Oda H, Sakamoto S, Yang Y, Sablier M. (2021). Paper fragments from the Tibetan Samye Monastery: Clues for an unusual sizing recipe implying wheat starch and milk in early Tibetan papermaking. *Journal of Archaeological Science: Reports*, 36, 102793. <https://doi.org/10.1016/j.jasrep.2021.102793>
- Han B, Vial J, Inaba M, Sablier M. (2017). Analytical characterization of East Asian handmade papers: A combined approach using Py-GCxGC/MS and multivariate analysis. *J. Anal. Appl. Pyrolysis*, 127, 150-158. <https://doi.org/10.1016/j.jaap.2017.08.013>
- Han B, Vial J, Sakamoto S, Sablier M. (2019). Identification of traditional East Asian handmade papers through the multivariate data analysis of pyrolysis-GC/MS data. *Analyst*, 144(4), 1230-1244. <https://doi.org/10.1039/C8AN01898G>
- Han B, Vilmont L-B, Kim H-J, Lavédrine B, Sakamoto S, Sablier M. (2021). Characterization of Korean handmade papers collected in a Hanji reference book. *Herit. Sci.*, 9(1), 96. <https://doi.org/10.1186/s40494-021-00570-9>
- Haugan E, Holst B. (2014). Flax look - alike: Pitfalls of ancient plant fibre identification. *Archaeometry*, 56(6), 951-960. <https://doi.org/10.1111/arcm.12054>
- Helman-Ważny A. (2016). More than meets the eye: Fibre and Paper Analysis of the Chinese Manuscripts from the Silk Roads. *STAR: Science & Technology of Archaeological Research*, 2(2), 127-140. <https://doi.org/10.1080/20548923.2016.1207971>
- Islam A, Sarkanen K V. (1993). The Isolation and Characterization of the Lignins of Jute (*Corchorus capsularis*). *Holzforschung*, 47(2), 123-132. <https://doi.org/10.1515/hfsg.1993.47.2.123>
- Kvavadze E, Bar-Yosef O, Belfer-Cohen A, Boaretto E, Jakeli N, Matskevich Z, Meshveliani T. (2009). 30,000-year-old wild flax fibers. *Science*, 325(5946), 1359-1359. <https://doi.org/10.1126/science.1175404>
- Kwon H. (2007). The dollarization of Vietnamese ghost money. *Journal of the Royal Anthropological Institute*, 13(1), 73-90. <https://doi.org/10.1111/j.1467-9655.2007.00414.x>
- Lebedev A T, Polyakova O V, Artaev V B, Mednikova M B, Anokhina E A. (2021). Comprehensive two - dimensional gas chromatography - high resolution mass spectrometry with complementary ionization methods in the study of 5000 - year - old mummy. *Rapid Commun. Mass Spectrom.*, 35(8), e9058. <https://doi.org/10.1002/rcm.9058>
- Lima C F, Barbosa L C A, Marcelo C R, Silvério F O, Colodette J L. (2008). Comparison between analytical pyrolysis and nitrobenzene oxidation for determination of syringyl/guaiacyl ratio in Eucalyptus spp. lignin. *BioResources*, 3(3), 701-712.
- Lukesova H, Holst B. (2021). Is Cross - Section Shape a Distinct Feature in Plant Fibre Identification? *Archaeometry*, 63(1), 216-226. <https://doi.org/10.1111/arcm.12604>
- Marques G, Rencoret J, Gutiérrez A, Del Rio J C. (2010). Evaluation of the chemical composition of different non-woody plant fibers used for pulp and paper manufacturing. *Open Agriculture Journal*, 4(2), 93-101. <https://doi.org/10.2174/1874331501004010093>
- Martoglio P A, Bouffard S P, Sommer A J, Katon J E, Jakes K A. (1990). Unlocking the secrets of the past: the analysis of archaeological textiles and dyes. *Anal. Chem.*, 62(21), 1123A-1128A. <https://doi.org/10.1021/ac00220a002>
- McCreery J L. (1990). Why don't we see some real money here? Offerings in Chinese religion. *Journal of Chinese Religions*, 18(1), 1-24. <https://doi.org/10.1179/073776990805307982>

- Nacci T, Sabatini F, Cirrincione C, Degano I, Colombini M P. (2022). Characterization of textile fibers by means of EGA-MS and Py-GC/MS. *J. Anal. Appl. Pyrolysis*, 105570. <https://doi.org/10.1016/j.jaap.2022.105570>
- Nanayakkara B, Riddell M, Harrington J. (2016). Screening of juvenile *Pinus radiata* wood by means of Py-GC/MS for compression wood focussing on the ratios of p-hydroxyphenyl to guaiacyl units (H/G ratios). *Holzforschung*, 70(4), 313-321. <https://doi.org/10.1515/hf-2015-0068>
- Netzel K. (2019). *Untersuchung von Lignin aus Papierabwässern mittels Py-GCxGC/TOF-MS und Ofenpyrolyse* [Universität Wuppertal, Fakultät für Mathematik und Naturwissenschaften].
- Nunes C A, Lima C F, Barbosa L C, Colodette J L, Gouveia A, Silvério F O. (2010). Determination of Eucalyptus spp lignin S/G ratio: A comparison between methods. *Bioresour. Technol.*, 101(11), 4056-4061. <https://doi.org/10.1016/j.biortech.2010.01.012>
- Ohra-Aho T, Gomes F, Colodette J, Tamminen T. (2013). S/G ratio and lignin structure among Eucalyptus hybrids determined by Py-GC/MS and nitrobenzene oxidation. *J. Anal. Appl. Pyrolysis*, 101, 166-171. <https://doi.org/10.1016/j.jaap.2013.01.015>
- Okamoto S, Honda T, Miyakoshi T, Han B, Sablier M. (2018). Application of pyrolysis-comprehensive gas chromatography/mass spectrometry for identification of Asian lacquers. *Talanta*, 189, 315-323. <https://doi.org/10.1016/j.talanta.2018.06.079>
- Pandey S. (2007). Ramie fibre: part I. Chemical composition and chemical properties. A critical review of recent developments. *Textile Progress*, 39(1), 1-66. <https://doi.org/10.1080/00405160701580055>
- Perruchini E, Pinault G-J, Sablier M. (2022). Exploring the potential of pyrolysis-comprehensive two-dimensional gas chromatography/mass spectrometry in the characterization of Chinese inks of ancient manuscripts. *J. Anal. Appl. Pyrolysis*, 164, 105503. <https://doi.org/10.1016/j.jaap.2022.105503>
- Ramos L, Udo A T. (2009). Multidimensionality in gas chromatography: general concepts. *Comprehensive Analytical Chemistry*, 55, 3-14. [https://doi.org/10.1016/S0166-526X\(09\)05501-9](https://doi.org/10.1016/S0166-526X(09)05501-9)
- Sakamoto S, Okada Y. (2013). Paper Analysis and Paper History from Ancient Chinese Paper to Japanese Washi. 2013 International Conference on Culture and Computing,
- Scott J L. (2007). *For gods, ghosts and ancestors: The Chinese tradition of paper offerings* (Vol. 1). Hong Kong University Press.
- Seaman G. (1982). Spirit money: an interpretation. *Society for the Study of Chinese Religions Bulletin*, 10(1), 80-91. <https://doi.org/10.1179/073776982805308395>
- Shedrinsky A M, Wampler T P, Indictor N, Baer N S. (1989). Application of analytical pyrolysis to problems in art and archaeology: a review. *J. Anal. Appl. Pyrolysis*, 15, 393-412. [https://doi.org/10.1016/0165-2370\(89\)85050-8](https://doi.org/10.1016/0165-2370(89)85050-8)
- Shi J I, Li T. (2013). Technical investigation of 15th and 19th century Chinese paper currencies: Fiber use and pigment identification. *Journal of Raman Spectroscopy*, 44(6), 892-898. <https://doi.org/10.1002/jrs.4297>
- Silva T C F, Gomide J L, Santos R B. (2012). Evaluation of chemical composition and lignin structural features of *Simarouba versicolor* wood on its pulping performance. *BioResources*, 7(3), 3910-3920.
- Tranchida P Q, Salivo S, Franchina F A, Mondello L. (2015). Flow-modulated comprehensive two-dimensional gas chromatography combined with a high-resolution time-of-flight mass spectrometer: A proof-of-principle study. *Anal. Chem.*, 87(5), 2925-2930. <https://doi.org/10.1021/ac5044175>

- Umamaheswaran R, Dutta S, Khan M A, Bera M, Bera S, Kumar S. (2022). Identification of Chitin in Pliocene Fungi Using Py-GC × GC-TOFMS: Potential Implications for the Study of the Evolution of the Fungal Clade in Deep Time. *Anal. Chem.*, 94(4), 1958-1964. <https://doi.org/10.1021/acs.analchem.1c03143>
- Van Erven G, de Visser R, Merckx D W, Strolenberg W, de Gijssel P, Gruppen H, Kabel M A. (2017). Quantification of lignin and its structural features in plant biomass using <sup>13</sup>C lignin as internal standard for pyrolysis-GC-SIM-MS. *Anal. Chem.*, 89(20), 10907-10916. <https://doi.org/10.1021/acs.analchem.7b02632>
- Wang T-P, Li H, Yuan J-M, Li W-X, Li K, Huang Y-B, Xiao L-P, Lu Q. (2021). Structures and pyrolytic characteristics of organosolv lignins from typical softwood, hardwood and herbaceous biomass. *Industrial Crops and Products*, 171, 113912. <https://doi.org/10.1016/j.indcrop.2021.113912>
- Wiesner D J. (1887). *Die mikroskopische Untersuchung des Papiers mit besonderer Berücksichtigung der ältesten orientalischen und europäischen Papiere, von Dr. Julius Wiesner*. Hof-und Staatsdruckerei.

## Figure captions

**Fig. 1** The archaeological paper offering samples from Astana cemetery. (i) offcut of paper offerings from the tomb of 72TAM184:5; (ii) offcut of paper offerings from the tomb of 72TAM184:2; (iii) remains of paper offerings from the tomb of 73TAM501:108; (iv) paper offerings from the tomb of 73TAM518:9; (v) general view of paper offerings from Astana Cemeteries. scale bar in (i)-(ii) is 1 cm, in (v) is 10 cm.

**Fig. 2** Micrograph of paper offerings from Astana tombs. (i) 72TAM184:5, (a)-(b); (ii) 72TAM184:2, (c)-(f); (iii) 72TAM501:108, (g)-(h); (iv) 73TAM518:9, (i)-(l).

**Fig. 3** Microscopic morphological features of the stained fibers of samples (i)-(iv), scale bar=20 μm. More microscopic pictures examined in the course of the present work can be found in Figure S3, Supplementary information.

**Fig. 4** (a) An example of a 2D chromatogram resulting from the pyrolysis of a handmade reference jute paper showing the separation of the lignocellulose components, (b) the grouping features of different series of lignin monomers (H,G,S monomers with different side-chains) in the 2D chromatogram space. In (a), the cellulose region represents a region mainly of cellulose pyrolysis products, and the lignin region represents a region mainly of lignin pyrolysis products. In (b), H, G, and S represent different types of lignin monomers, while alkyl, alkenyl, keto-/aldehyde/enol represent side-chain constituents. The full 2D chromatographic space is

shown in Figure S8. In (a) and (b), the yellow blobs represent the lignin monomers, and for compound identification, refer to Table 1 and Figure S9.

**Fig. 5** Measured S/G ratio by Py-GCxGC/MS for the reference samples of ramie, flax, hemp, jute and the four Astana samples (i)-(iv).

**Fig. 6** Dendrogram of the hierarchical clustering of reference paper samples and Astana paper samples using normalized data of the 27 lignin markers reported in Table 1.

**Fig. 7** PCA (weighted as 1/STD) of the reference paper samples and the Astana paper samples using normalized values for the 27 lignin markers (Table 1). In (a), R: ramie, F: flax, J: jute, H: hemp, (i)-(iv): the four Astana paper samples; in (b), H/G/S represents the three types of lignin monomers.

**Fig. 8** PCA of the reference paper samples and the Astana paper samples using normalized values for the only G-type and S-type lignin markers (Table 1), weighted as 1/STD. In (a), R: ramie, F: flax, J: jute, H: hemp, (i)-(iv): the four Astana paper samples; in (b), H/G/S represents the three types of lignin monomers.